Progress in Flight Physics **3** (2012) 471-482

MODEL REDUCTION AND CONTROL OF A SEPARATING BOUNDARY-LAYER FLOW

U. Ehrenstein[1], P.-Y. Passaggia[1], and F. Gallaire[2]

[1]IRPHÉ, Aix-Marseille Université
Rue Joliot-Curie 49, F-13384 Marseille Cedex 13, France

[2]Lab. J. A. Dieudonné, Université de Nice-Sophia
Antipolis, Parc Valrose, F-06108 Nice Cedex 02, France

The possibility of model reduction using global modes is readdressed, aiming at the controlling of a globally unstable separation bubble induced by a bump geometry. A combined oblique and orthogonal projection approach is proposed to design an estimator and controller in a Riccati-type feedback setting. The dimension of the reduced-order model is optimized using an input–output criterion. The full-state linear instability dynamics is shown to be successfully controlled by the feedback coupling with controllers of moderate degrees of freedom.

1 INTRODUCTION

Separated boundary layer flows are ubiquitous in both external and internal practical flows, like the rear of a vehicle or wings at high incidence. They are often associated with strong instabilities with a broad frequency spectrum which are still not entirely understood, despite a longstanding theoretical, numerical, and experimental effort [1, 2]. As an archetype configuration, the backward-facing step, showing various phenomena associated with flow separation, has been often considered for the purpose of control. Feedback and instantaneous control strategies have been developed for this flow case, for instance, to reduce the recirculation bubble length in the laminar flow case [3] or to increase mixing in turbulent flow [4]. In the present paper, a recirculation region created by a boundary layer encountering a shallow bump is considered. For the same flow geometry, the instability behavior has been analyzed recently in [5], using the numerical global instability setting. This flow configuration and the associated numerical model are appropriate for feedback control in the context of linear systems approach to flow control, which has found a lot of attention during the last decade (see the review [6]).

Given the extensive degrees of freedom of the flow dynamics, dynamical system control theory can, however, hardly be applied to the full flow state and the issue of model reduction is intimately related to the control issue. Very recently, the input–output formulation of flow control problems has led to promising results with regard to model reduction and it has been successfully applied to the control of channel flow [7] or the flat-plate boundary layer [8]. The projection basis in this approach is optimal with respect to observability and controllability for the specific actuators and sensors considered. Some attempts have also been made to exploit in the model reduction procedure the underlying physical mechanisms of the flow instability and, in particular, to use the global modes for projection. This approach has been applied to a shallow cavity [9] with some success. Very recently, the reliability of model reduction using global modes has been questioned in [10], considering an open square cavity. The performance of the resulting compensator obtained via bi-orthogonal projection for this non-normal flow case is shown in [10] to be less efficient, in comparison with models based on proper orthogonal decomposition and balanced modes. However, while the latter methods are designed to optimally reproduce the input-output behavior, they necessitate the computation and the approximation in a time-stepping procedure of the Gramians associated with controllability and observability [11].

In the present work, the possibility of model reduction using global mode subspaces is readdressed by focusing on an alternative projection approach, which is optimal with regard to the spatial actuator structure.

2 FLOW CONFIGURATION AND NUMERICAL MODEL

The flow geometry considered herein is $0 \leq x \leq L$, $\eta(x) \leq y \leq H$, with $\eta(x)$ the lower boundary containing a bump with height h. The same geometry has been used in [5, 12] and the basic flow state exhibits an elongated recirculation bubble at the rear of the bump depicted in Fig. 1 for a bump height $h = 2$. This flow state has been computed as a nonlinear equilibrium solution of the stationary Navier–Stokes system

$$\mathbf{f}(\mathbf{u}, p, \mathrm{Re}) = \left[-(\mathbf{u} \cdot \nabla)\mathbf{u} - \nabla p + \frac{1}{\mathrm{Re}} \nabla^2 \mathbf{u} \,;\; \nabla \cdot \mathbf{u} \right] = \mathbf{0} \,,$$

for the flow velocity $\mathbf{u} = (u, v)$ and pressure p. The domain length is $L = 300$ which has been shown in [5] to be large enough to avoid the influence of the outflow boundary on the flow dynamics. The domain height is $H = 30$ and it proved suitable to recover uniform flow consistent with the upper boundary condition $\mathbf{u} = (1, 0)$. The Reynolds number $\mathrm{Re} = \delta^* U_\infty / \nu$ is based on the displacement thickness of the Blasius profile $(U(y), 0)$ which is imposed at inflow

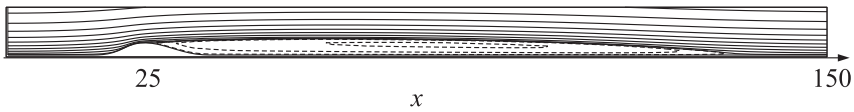

Figure 1 Streamlines in the vicinity of the wall boundary of steady flow state at $R = 590$ and for a bump height $h = 2$

and at outflow homogeneous Neumann boundary conditions for the flow velocity field $\mathbf{u}$ are prescribed. The system has been discretized using Chebyshev collocation in both the streamwise x direction and wall-normal y direction, together with an algebraic mapping transforming the physical domain into the Cartesian computational domain $[-1, 1] \times [-1, 1]$. To recover a steady equilibrium state, a quasi-Newton method together with an arclength continuation procedure has been used. Details about the solution procedure are provided in [5].

In the following, it is denoted $\mathbf{A}(\mathbf{u}_s, \mathrm{Re}) = D_{(\mathbf{u},p)}\mathbf{f}(\mathbf{u}_s, p_s, \mathrm{Re})$ the Jacobian matrix evaluated at basic equilibrium states $(\mathbf{u}_s, p_s)$. The dynamics of linear disturbances is, hence, governed by the system

$$\mathbf{E}\frac{d}{dt}\mathbf{q} = \mathbf{A}(\mathbf{u}_s, \mathrm{Re})\mathbf{q}, \quad \mathbf{E}\mathbf{q} = (u, v, 0)\,, \tag{1}$$

with $\mathbf{q} = (u, v, p)$ the linear flow disturbance. The pressure is given implicitly through the incompressibility condition which is imposed in the interior domain as well as on the boundary. Spurious pressure modes which are inherent when a Chebyshev discretization is used in a rectangular box [13] are eliminated through simple algebraic relations, similar to the procedure outlined in [14]. The matrix $\mathbf{A}(\mathbf{u}_s, \mathrm{Re})$ is, hence, nonsingular and $\mathbf{E}$ being the projection of the solution vector $\mathbf{q}$ onto the perturbation flow velocity components, system (1) may be integrated using multistep backward differentiation formulae (BDF), which are appropriate for the time-integration of differential-algebraic systems [15].

The stability of the basic steady state $(\mathbf{u}_s, p_s)$ is computed by considering the two-dimensional temporal modes $\mathbf{q} = \widehat{\mathbf{q}}(x, y)\; e^{-i\omega t}$, $\widehat{\mathbf{q}} = (\widehat{u}, \widehat{v}, \widehat{p})$, and, hence, according to (1), the eigenvalues ω_j and eigenvectors $\widehat{\mathbf{q}}_j$ are solution of

$$-i\omega_j \mathbf{E}\widehat{\mathbf{q}}_j = \mathbf{A}\widehat{\mathbf{q}}_j \tag{2}$$

with $\mathbf{A}$ the Jacobian matrix (the reference to the basis state $\mathbf{u}_s$ and Reynolds number is omitted). The resulting large eigenvalue problem is solved using large-scale Krylov subspace projections together with the Arnoldi algorithm and the stability for the recirculation bubble has been assessed in [5].

A grid with $N_x = 200$ collocation points in x and $N_y = 30$ collocation points in y is considered, which has proved in [5] to be sufficient to describe the instability dynamics. The Reynolds number is $\mathrm{Re} = 590$, for a bump height $h = 2$,

which is slightly above the threshold for the global dynamics analyzed in [5]. This latter work allowed to interpret the low-frequency oscillations of the recirculation bubble, which had been observed in direct numerical simulations [12], in terms of interaction of global modes. Here, the goal is to evaluate the possibility of feedback control of the underlying global instability dynamics.

Control, Estimation, and Modal Decomposition

Given the degrees of freedom of real full flow states, only a partial-state control approach is feasible in general and, hence, the flow state has to be estimated. A control device has to be designed which efficiently acts on the flow dynamics and sensors are implemented to measure significant flow quantities. In the present work, which aims at reassessing model reduction using global modes rather than providing realistic flow control, a divergence-free spatially localized volume force $\mathbf{B} = (B_x, B_y)$ has been chosen as actuator. The actuator has a Gaussian envelope and the two components are shown in Fig. 2.

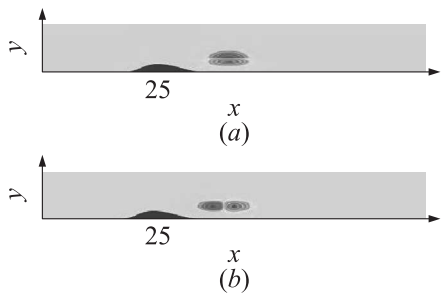

Figure 2 Actuator: (a) streamwise component B_x and (b) wall-normal component B_y

The flow is sensored by skin-friction measurements at several locations along the plate, starting approximately at the center of the steady flow recirculation bubble end extending to the outflow region of the computational domain. The measurements are collected in a vector $\mathbf{y}$ with components

$$y_i = \int_{x_i}^{x_i+\Delta x} \frac{\partial u}{\partial y}(x,0)\,dx\,, \quad i = 1, \cdots, 6$$

where $\Delta x = 20$ and $x_1 = 60$, $x_2 = 100$, $x_3 = 140$, $x_4 = 180$, $x_5 = 220$, $x_6 = 260$.

In the absence of the full knowledge of the state vector $\mathbf{q}$, a state estimate $\mathbf{q}_e$ is introduced, which mimics the unknown state vector: it is governed by the same dynamics, forced by the same control, but also forced by a restoring term $\mathbf{L}(\mathbf{y}_e - \mathbf{y})$ for the real measurements to be followed as exactly as possible. The optimal choice of this restoring estimator gain $\mathbf{L}$ as detailed below is also called Kalman filter [16]. In essence, the estimator receives the measurements, determines the estimated flow which is fed back by the controller. Adding the actuator $\mathbf{B}$ to system (1) and introducing a measurement operator $\mathbf{C}$, the coupling with the estimator and the controller gives rise to the system

$$\mathbf{E}\frac{d}{dt}\,\mathbf{q} = \mathbf{A}\mathbf{q} + \mathbf{B}\phi, \quad \mathbf{y} = \mathbf{C}\mathbf{q}\,; \tag{3}$$

$$\mathbf{E}\frac{d}{dt}\,\mathbf{q}_e = \mathbf{A}\mathbf{q}_e + \mathbf{B}_e\phi + \mathbf{L}(\mathbf{y}_e - \mathbf{y})\,, \quad \mathbf{y}_e = \mathbf{C}\mathbf{q}_e, \quad \phi = \mathbf{K}\mathbf{q}_e\,. \tag{4}$$

The operators $\mathbf{K}$ and $\mathbf{L}$ are called control gain and estimation gain, respectively. For the derivation of this setting and, more generally, for the application of linear systems approach to flow control, see the review [6] and the references therein.

The dimension of the dynamical system (4), called the compensator, should be as low as possible to provide immediate feedback control ϕ when receiving the flow measurement $\mathbf{y}$. Focusing on model reduction using global modes, the actuator $\mathbf{B}_e$ is sought for as the expansion of the physical actuator $\mathbf{B}$ into a set of eigenvectors, solution of the generalized matrix eigenvalue problem (2). The operators being real, the eigenvectors are complex conjugate pairs and

$$\mathbf{B}_e = \mathbf{E}\sum_{i=1}^{m}\left(\beta_j\widehat{\mathbf{q}}_j + \bar{\beta}_j\bar{\widehat{\mathbf{q}}}_j\right) \tag{5}$$

(the variables with the bar being the complex conjugate) with $\widehat{\mathbf{q}}_j$ solutions of (2). The operator $\mathbf{B}_e$ may equivalently be written in the real vectorspace

$$\mathbf{B}_e = \mathbf{E}\mathbf{V}\widehat{\mathbf{b}}, \quad \text{with} \quad \mathbf{V} = \left(\,\widehat{\mathbf{q}}_{1r}\;\widehat{\mathbf{q}}_{1i}\;\cdots\;\widehat{\mathbf{q}}_{mr}\;\widehat{\mathbf{q}}_{mi}\,\right), \tag{6}$$

the $n = 2m$ columns of the matrix $\mathbf{V}$ being the real parts $\widehat{\mathbf{q}}_{jr}$ and imaginary parts $\widehat{\mathbf{q}}_{jr}$ of the eigenvectors (for corresponding eigenvalues $\lambda_j = -i\omega_j$ with nonzero imaginary parts). Expanding the estimated flow state in terms of the eigenvectors $\mathbf{q}_e = \mathbf{V}\widehat{\mathbf{x}}$, the compensator (4) is written as the n-dimensional system

$$\frac{d}{dt}\,\widehat{\mathbf{x}} = \mathbf{\Lambda}\widehat{\mathbf{x}} + \widehat{\mathbf{b}}\phi + \widehat{\mathbf{L}}(\mathbf{y}_e - \mathbf{y})\,, \quad \mathbf{y}_e = \widehat{\mathbf{C}}\widehat{\mathbf{x}}\,, \quad \phi = \widehat{\mathbf{K}}\widehat{\mathbf{x}} \tag{7}$$

where $\widehat{\mathbf{C}} = \mathbf{C}\mathbf{V}$. The estimation gain and control gain in (4) are related to the corresponding operators in (7) through the relations $\mathbf{L} = \mathbf{V}\widehat{\mathbf{L}}$ and $\mathbf{K} = \widehat{\mathbf{K}}\mathbf{P}$. The operator $\mathbf{V}$ is defined in (6) and the expansion coefficients $\widehat{\mathbf{x}}$ of $\mathbf{q}_e = \mathbf{V}\widehat{\mathbf{x}}$ may be written $\widehat{\mathbf{x}} = \mathbf{P}\mathbf{q}_e$ for some operator $\mathbf{P}$, by making use of the bi-orthogonal property.

Assuming $\mathbf{y}_e = \mathbf{y}$ in (7), which corresponds to the so-called full information control, the gain matrix $\widehat{\mathbf{K}}$ is computed by solving an algebraic Riccati equation, associated with the minimization of the functional (for time-horizon $T \to \infty$)

$$\mathcal{J} = \frac{1}{2}\int_0^T \widehat{\mathbf{x}}^T\mathbf{V}^T\mathbf{W}\mathbf{V}\widehat{\mathbf{x}}\,dt + \frac{l^2}{2}\int_0^T \phi^2\,dt\,.$$

The first term of the right-hand side is the projected flow energy, with $\mathbf{W}$ a diagonal matrix with the appropriate weights for the numerical quadrature of the integral $\int(u^2+v^2)\,dxdy$ in the flow domain and the parameter l^2 puts a bound on the control ϕ. Subtracting (4) from (3) and assuming that the error between the real and the projected actuator $\widetilde{\mathbf{B}} = \mathbf{B} - \mathbf{B}_e \approx 0$, $\widehat{\mathbf{L}}$ is again computed as a feedback gain matrix minimizing the energy of the projected state estimation error. The procedure is outlined in the review [6] and it has been used in [8, 9, 17], among others. In this whole section, the only requirement was to decompose all vectors on an invariant subspace, but the choice of the direction of projection (either orthogonal or oblique) remains open.

3 BI-ORTHOGONAL AND LEAST-SQUARE PROJECTION

Performing several shifts in the Arnoldi algorithm (cf. [18]), a large part of the spectrum has been computed with 900 modes in the complex half plane $\omega_r > 0$ which are depicted in Fig. 3. There are unstable eigenvalues with $\omega_i > 0$ and the associated dynamics has been addressed in [5]. The conventional projection procedure for nonnormal problems uses the bi-orthogonal property $\langle \widehat{\mathbf{q}}_k^+, \mathbf{E}\widehat{\mathbf{q}}_j \rangle = \delta_{kj}$ with respect to the Hermitian inner product, the adjoint modes $\hat{\mathbf{q}}_k^+$ being solution of the generalized eigenvalue problem

$$i\omega_k \mathbf{E}\widehat{\mathbf{q}}_k^+ = \mathbf{A}^T \widehat{\mathbf{q}}_k^+$$

of the adjoint system with $\mathbf{A}^T$ merely the transposed discretized operator. The most unstable eigenmode, labelled *1* in Fig. 3 is depicted in Fig. 4*a* whereas

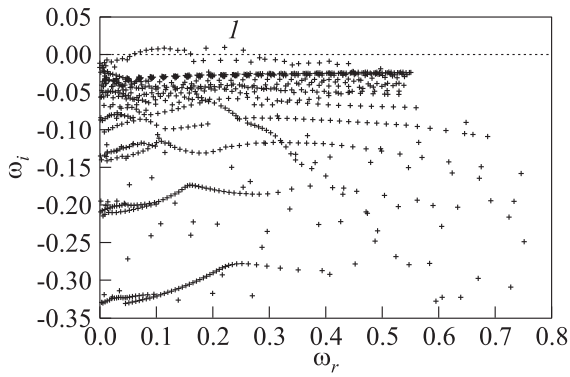

Figure 3 Spectrum in the half plane $\omega_r > 0$ with $m = 900$ eigenvalues

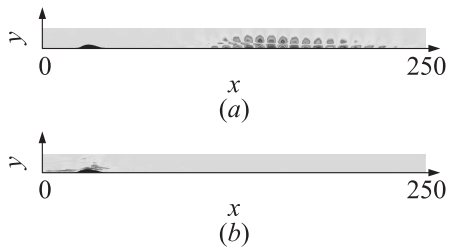

Figure 4 Streamwise components of the most unstable eigenmode (labeled *1* in Fig. 3) (*a*) and of the associated adjoint eigenfunction (*b*)

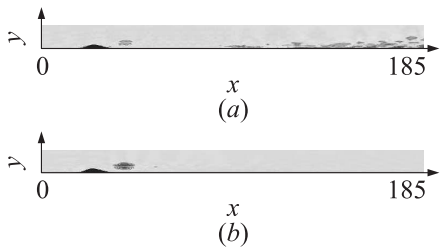

Figure 5 Streamwise component B_x of the projected actuator: (*a*) bi-orthogonal projection, $m = 900$; and (*b*) least-square projection, $m_u = 13, m_s = 887$

the associated adjoint eigenvector structure is given in Fig. 4*b*. As discussed, for instance in [19], the clear separation in space between the direct and adjoint eigenfunction is associated with the strong streamwise nonnormality.

Using the bi-orthogonal property, the coefficients in the expansion (5) can by computed (or, equivalently, the $n = 2m$ coefficients in the projection (6)). The projected operator $\mathbf{B}_e$ with $m = 900$ is shown in Fig. 5*a*. While the volume forcing structure nearby the bump is reasonably reproduced (cf. Fig. 2), the projected operator is far from being localized, given its structure extending downstream. This reflects the strong nonnormality, the adjoint modes localized upstream providing nonzero inner-products with the actuator, whereas the associated dominant direct modes are located downstream the bump. The error between the real and the reduced actuator appears to be a major difficulty in this *a priori* model reduction approach, contrary to the input–output analysis for flow control based on observability and controllability operators. In this latter approach, which has recently been applied, for instance, to the control of channel flow in [7] or the flat-plate boundary layer in [8], the actuator $\mathbf{B}$ enters directly into the construction of the so-called balanced modes used for reduction.

Combined Bi-Orthogonal and Least Squares Projection

In order to minimize the error $\widetilde{\mathbf{B}}$ between the real and the projected actuator, a least-square procedure is proposed as follows. The matrix $\mathbf{V}$ in (6) contains the real and imaginary parts of the set of eigenvectors and the block with the m_u unstable eigenvectors are separated from the block containing the m_s stable ones, by writing

$$\mathbf{V} = \left(\mathbf{V}_u \; \mathbf{V}_s \right) .$$

To avoid that the projection error triggers a global instability dynamics, the projection of $\mathbf{B}$ on the unstable eigenvectors is first performed by bi-orthogonality, giving rise to

$$\mathbf{B}_u = \mathbf{E}\mathbf{V}_u\widehat{\mathbf{b}}_u$$

(note that in the present case, $m_u = 13$). Writing

$$\mathbf{B}_e = \mathbf{B}_u + \mathbf{B}_s\,, \tag{8}$$

the projection on the stable part of the spectrum $\mathbf{B}_s = \mathbf{V}_s\widehat{\mathbf{b}}_s$ is computed as solution of the least-square projection with

$$||\mathbf{V}_s\widehat{\mathbf{b}}_s - (\mathbf{B} - \mathbf{B}_u)||^2 = \min_{\widehat{y}} ||\mathbf{V}_s\widehat{y} - (\mathbf{B} - \mathbf{B}_u)||^2$$

(with $||\mathbf{g}||^2 = \mathbf{g}^T\mathbf{W}\mathbf{g}$ the discrete version of the domain integral $\int (g_x^2 + g_y^2)\,dxdy$ for a volume function $g = (g_x, g_y)$).

With the decomposition (8), the projection error is orthogonal to the set of stable eigenmodes for the modal subspace considered and it has no contribution with respect to the unstable eigenmodes. This projection procedure gives rise to $\mathbf{B}_e$ depicted in Fig. 5*b* and the actuator is seen to be very close to the physical one.

The projection has been performed considering $m = 900$ complex eigenvectors and the associated reduced system in the real vectorspace (7) is of dimension $n = 2m = 1800$. Note that the full state system, that is, the differential-algebraic system (1), is of dimension 18,000 for the discretization considered here. The dimension of the reduced system is far from being optimized and some criterion has to be applied to assess the amount of information contained in the modes, with regard to the control issue. This point has been addressed, for instance, in [8, 10]. The idea is to quantify the output $\mathbf{y} = \mathbf{C}\mathbf{q}$ for harmonic actuation inputs $\phi = e^{i\omega t}$ for the (complex) system

$$\mathbf{E}\frac{d}{dt}\mathbf{q} = \mathbf{A}\mathbf{q} + \mathbf{B}_j e^{i\omega t}$$

and, consequently, $\mathbf{y} = \mathbf{C}\left(i\omega\mathbf{E} - \mathbf{A}\right)^{-1}\mathbf{B}_j e^{i\omega t}$, with $\mathbf{B}_j = \beta_j\mathbf{E}\hat{\mathbf{q}}_j$ the component of the projected actuator with respect to the eigenvector $\mathbf{q}_j$. It may be shown (see [8]) that

$$|\mathbf{y}| \leq \frac{|\mathbf{C}_j||\beta_j|}{|\mathcal{R}e(\lambda_j)|} = \Gamma_j, \tag{9}$$

with $\mathbf{C}_j = \mathbf{C}\widehat{\mathbf{q}}_j$ the skin friction measurements of the global mode and $\lambda_j = -i\omega_j$ are the eigenvalues. The quantity Γ_j is convenient to provide the hierarchy of the modes with respect to controllability and observability.

4 CONTROL RESULTS

Putting together the plant (3) and the compensator (7), one recovers the system

$$\mathbf{E}\frac{d}{dt}\,\mathbf{q} = \mathbf{A}\mathbf{q} + \mathbf{B}\phi\,, \quad \mathbf{y} = \mathbf{C}\mathbf{q}\,;$$
$$\frac{d}{dt}\,\widehat{\mathbf{x}} = \left(\mathbf{\Lambda} + \widehat{\mathbf{b}}\widehat{\mathbf{K}} + \widehat{\mathbf{L}}\widehat{\mathbf{C}}\right)\widehat{\mathbf{x}} - \widehat{\mathbf{L}}\mathbf{y}\,;$$
$$\phi = \widehat{\mathbf{K}}\widehat{\mathbf{x}}\,.$$

The double-projection as exposed in the previous section has been performed for the actuator **B** depicted in Fig. 2, that is the bi-orthogonal projection for the unstable modes followed by the least-square projection on the stable modes, for the set of $m = 900$ eigenvectors (with eigenvalues $\omega_r > 0$ depicted in Fig. 3) giving rise to a real vector $\widehat{\mathbf{b}}$ of dimension 1800. Then, the selection criterion has been applied to select the components for decreasing Γ_j defined in (9). According to this criterion, estimators (that is, the corresponding control and estimation gains) have been computed with dimensions 1200, 400, and 100.

As initial perturbation of the flow, a volume force of Gaussian-type, similar to the actuator structure but localized upstream of the bump near the entry of the flow domain, has been applied at $t = 0$. The solid line in Fig. 6 shows the uncontrolled flow dynamics exhibiting a strong transient energy growth followed by the beating behavior which has been analyzed in [5] in terms of the interaction between the global unstable modes. The flow structure is shown in Fig. 7 at

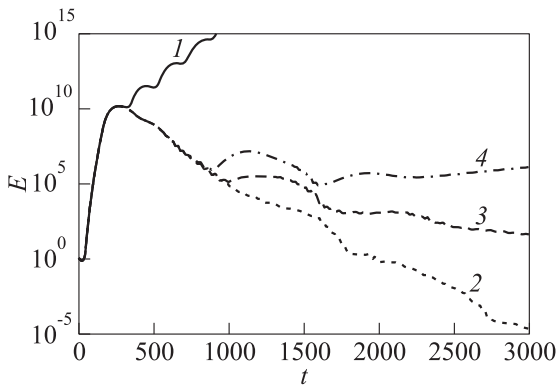

Figure 6 Flow energy (normalized by $E(0)$) as function of time: *1* — uncontrolled case; *2* — control, estimator of dimension 1200; *3* — estimator of dimension 400; and *4* — estimator of dimension 100

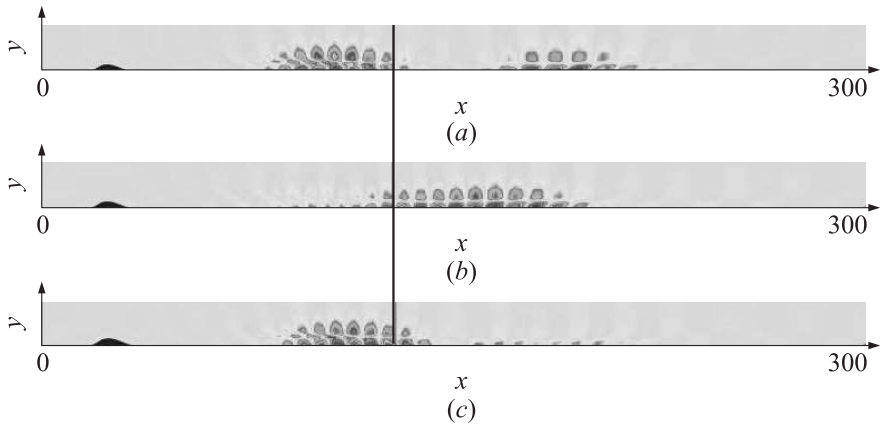

Figure 7 Streamwise velocity component of the uncontrolled flow at $t = 350$ (a), 485 (b), and 550 (c). The vertical line shows the location of the reattachment point of the basic flow recirculation bubble. The amplitude of the perturbation is normalized for each snapshot

$t = 350$, 485, and 550, illustrating the periodic (with period $T \approx 200$) regeneration of the perturbation within the recirculation bubble.

The control is shown to have no impact on the transient energy growth up to $t = 200$. Indeed, the controller can start to act only after the initial disturbance (localized upstream) has reached the first sensor, the first skin-friction measurement starting at $x = 60$. Then, up to a time of $t \approx 700$, the controllers act similarly, regardless of their dimensions. The long-time behavior is, however, different, the feedback with the estimator of dimension 1200 leading to vanishing flow. The estimator of dimension 400 appears to be sufficiently reliable to

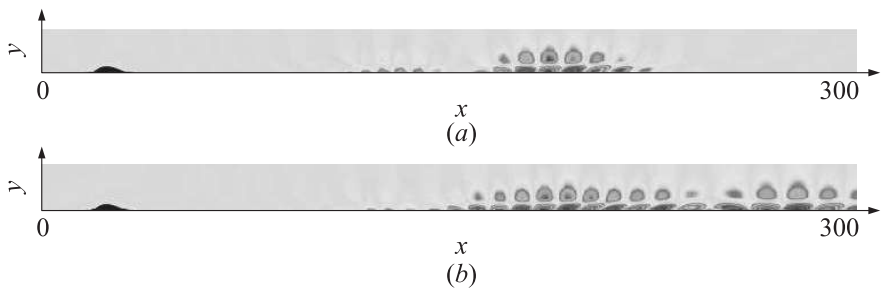

Figure 8 Streamwise velocity component of the controlled flow at $t = 350$ (a) and 550 (b). The amplitude of the perturbation is normalized for each snapshot

stabilize the flow, whereas the dimension 100 is too low to prevent an onset of small energy increase for $t > 1500$. The controlled flow structure is shown in Fig. 8, for the control with the estimator of dimension 1200. Clearly, the control prevents the regeneration of the perturbation which is washed downstream and eventually vanishes.

5 CONCLUDING REMARKS

When adopting a dynamical system approach for flow control, the global modes appear naturally as a possible projection basis for model reduction. While these modes reproduce the instability physics, they may, however, not be efficient from the input-output viewpoint of system theory which uses the controllability and observability operators. In this latter case, the actuator designed to control the flow as well as the sensor operator are part of the formulation, which, however, relies on the time-history of the dynamics. In the *a priori* model reduction using global modes, one critical issue is here shown to be the error between the real and the projected actuator. For the flow estimation to be reliable, this error must not trigger global instabilities and it should be as small as possible. For a given set of eigenmodes, this can be achieved by successively applying a bi-orthogonal projection with respect to the unstable global modes and a least-square projection on the subspace formed by the stable modes. An input–output kind of selection criterion based on the output for harmonic actuation inputs can subsequently be applied to optimize the dimension of the reduced-order compensator. The reliability of this approach has been tested, by coupling the compensator to the large-scale differential-algebraic system for the instability dynamics of a separation bubble. Fairly low-dimensional controllers, with few hundreds of degrees of freedom, successfully control the unstable flow dynamics. Note that for the present flow case, conventional bi-orthogonal projection (used in [9] for the control of a shallow cavity flow) necessitates a compensator of dimension twice as high to achieve equivalent control performance, as shown in [20].

REFERENCES

1. Alam, M., and N. D. Sandham. 2000. Direct numerical simulation of 'short' laminar separation bubbles with turbulent reattachment. *J. Fluid Mech.* 410:1–28.
2. Rist, U., and U. Maucher. 2002. Investigations of time-growing instabilities in laminar separation bubbles. *Eur. J. Mech. B/Fluids* 21:495–509.
3. Choi, H., M. Hinze, and K. Kunisch. 1999. Instantaneous control of backward-facing step flows. *Appl. Numer. Math.* 31:133–58.

4. Kang, S., and H. Choi. 2002. Suboptimal feedback control of turbulent flow over a backward-facing step. *J. Fluid Mech.* 463:201–27.
5. Ehrenstein, U., and F. Gallaire. 2008. Two-dimensional global low-frequency oscillations in a separating boundary-layer flow. *J. Fluid Mech.* 614:315–27.
6. Kim, J., and R. Bewley. 2007. A linear systems approach to flow control. *Annu. Rev. Fluid Mech.* 39:383–417.
7. Ilak, M., and C. W. Rowley. 2008. Modeling of transitional channel flow using balanced proper orthogonal decomposition. *Phys. Fluids* 20:034103.
8. Bagheri,S., L. Brandt, and D. Henningson. 2009. Input–output analysis, model reduction and control of the flat-plate boundary layer. *J. Fluid Mech.* 620:263–98.
9. Åkervik, E., J. Hœpffner, U. Ehrenstein, and D. S. Henningson. 2007. Optimal growth, model reduction and control in a separated boundary-layer flow using global eigenmodes. *J. Fluid Mech.* 579:305–14.
10. Barbagallo, A., D. Sipp, and P. J. Schmid. 2009 (in press). Closed-loop control of an open cavity flow using reduced-order models. *J. Fluid Mech.*
11. Rowley, C. W. 2005. Model reduction for fluids using balanced proper orthogonal decomposition. *Intl J. Bifurc. Chaos* 15:997–1013.
12. Marquillie, M., and U. Ehrenstein. 2003. On the onset of nonlinear oscillations in a separating boundary-layer flow. *J. Fluid Mech.* 490:169–88.
13. Peyret, R. 2002. *Spectral methods for incompressible flows.* Springer.
14. Ehrenstein, U., and F. Gallaire. 2005. On two-dimensional temporal modes in spatially evolving open flows: The flat-plate boundary layer. *J. Fluid Mech.* 536:209–18.
15. Kunkel, P., and V. Mehrmann. 2006. *Differential-alebraic equations.* EMS Textbooks in Mathematics.
16. Hœpffner, J., M. Chevalier, T. R. Bewley, and D. S. Henningson. 2005. State estimation in wall-bounded flow systems. Part I: Laminar flows. *J. Fluid Mech.* 534:263–94.
17. Barbagallo, A., D. Sipp, L. Jacquin, and P. J. Schmid. 2008. Control of an incompressible cavity flow using a reduced model based on global modes. AIAA Paper No. 2008-3904.
18. Nayar, O., and U. Ortega. 1993. Computation of selected eigenvalues of generalized eigenvalue problems. *J. Comput. Phys.* 108:8–14.
19. Chomaz, J.-M. 2005. Global instabilities in spatially developing flows: Non-normality and nonlinearity. *Annu. Rev. Fluid Mech.* 37:357–92.
20. Ehrenstein, U., P.-Y. Passaggia, and F. Gallaire. 2010. Control of a separated boundary layer: Reduced-order modeling using global modes revisited. *Theor. Comput. Fluid Dyn.* online: DOI 10.1007/s00162–010–0195–5.